

1 **The effect of inclusion of inlets in dual drainage modelling**

2 Tsang-Jung Chang^{1,2}, Chia-Ho Wang¹, Albert S. Chen^{3,*}, Slobodan Djordjević³

3 ¹ Department of Bioenvironmental Systems Engineering, National Taiwan University, Taipei,
4 Taiwan

5 ² Hydrotech Research Institute, National Taiwan University, Taipei, Taiwan

6 ³ Centre for Water Systems, College of Engineering, Mathematics and Physical Sciences,
7 University of Exeter, Exeter, United Kingdom

8 **Abstract**

9 In coupled sewer and surface flood modelling approaches, the flow process in gullies
10 is often ignored although the overland flow is drained to sewer network via inlets and
11 gullies. Therefore, the flow entering inlets is transferred to the sewer network
12 immediately, which may lead to a different flood estimation than the reality. In this
13 paper, we compared two modelling approach with and without considering the flow
14 processes in gullies in the coupled sewer and surface modelling. Three historical
15 flood events were adopted for model calibration and validation. The results showed
16 that the inclusion of flow process in gullies can further improve the accuracy of urban
17 flood modelling.

18 **Keywords:** Coupled 1D/2D flood model; Dynamic flow interaction; Model
19 comparison; Overland flow; Roof drainage; Storm sewer flow.

20 **1 Introduction**

21 Flooding is a major hazard in many urban areas that leads to significant damage to
22 properties and disruption of services. Hydraulic modelling is the key for better
23 understanding of flood dynamic such that enhanced adaptation measures can be
24 applied for disaster risk reduction (DRR). For most modern cities, storm sewer
25 networks are built to manage surface water caused by local rainfall. However, the
26 cost for the construction and maintenance of drainage networks is expensive such
27 that a standard between 1 in 1 to 1 in 30 years (Balmforth et al., 2006; Bloomberg

Please cite: *Chang T-J, Wang C-H, Chen AS, Djordjevic S (2018) The effect of inclusion of inlets in dual drainage modelling, Journal of Hydrology. Accepted.*

28 and Strickland, 2012; BSI, 2008; CIWEM UDG, 2016) is often used for designing
29 sewer systems. To evaluate the consequence of flooding due to extreme weather
30 conditions that are beyond the design standard, one-dimensional (1D) sewer flow
31 models (SFM) are widely adopted to examine the performance of drainage systems
32 for dealing with intense rainfall (Arnbjerg-Nielsen, 2008; Rossman, 2010).

33 To better describe the movement of surcharge flow from sewer networks, instead of
34 using simplified depth-volume functions, overland flow models (OFMs) are
35 introduced to simulate the runoff dynamic on the ground surface. The approach
36 coupling of SFM and OFM is regarded as the Dual Drainage approach (Djordjević et
37 al., 1999) that can be either a combination of 1D SFM and 1D OFM (Leandro et al.,
38 2009), or a combination of 1D SFM and two-dimensional (2D) OFM (Chen et al.,
39 2007; Hsu et al., 2002). Each of these approaches has advantages and
40 disadvantages (Allitt et al., 2009). In the last decade, coupled 1D SFM and 2D OFM
41 have been widely applied to urban flood modelling (Jahanbazi and Egger, 2014;
42 Russo et al., 2015; Seyoum et al., 2012; Vojinovic and Tutulic, 2009). Recently,
43 Leandro and Martins (2016) coupled 2D OFM with 1D SFM (SWMM 5.1) using
44 dynamic link libraries that avoids changing the source code in SWMM. Martins et al.
45 (2017) compared three approaches that were all coupled to the same 1D SFM to
46 analyse the differences in modelling results using the full shallow water equations,
47 the local inertial equations and the diffusive wave equations as the 2D OFM.

48 In our previous study (Chang et al., 2015), we compared six combinations of 1D
49 SFM and 2D OFM in urban flood modelling, including (1) 2D OFM only; (2) 2D OFM
50 with rainfall reduction or infiltration rate; (3) Combined SFM/OFM; (4) Coupled
51 SFM/OFM; (5) Coupled OFM/SFM; and (6) Mixed SFM/OFM and OFM/SFM
52 coupling. Details of these modelling approaches are provided in Chang et al. (2015).

Please cite: *Chang T-J, Wang C-H, Chen AS, Djordjevic S (2018) The effect of inclusion of inlets in dual drainage modelling, Journal of Hydrology. Accepted.*

53 The results showed that the bidirectional interaction between the sewer network and
54 the ground surface must be included in modelling to provide more accurate
55 estimations (i.e. approaches (4)-(6)). Furthermore, the interaction between the two
56 systems may vary because different land cover conditions have different
57 mechanisms. For example, if rainfall on a flat roof is collected and drained directly to
58 the sewer network then the downstream network may surcharge due to high
59 discharge into the system and the coupled SFM/OFM approach is adequate to
60 simulate the condition that the sewer flow returns to the surface. On the other hand,
61 the excess runoff from the precipitation falling on pervious area may propagate along
62 terrain until reaching an inlet that drains the overland flow into the sewer system,
63 which is better reflected by the coupled OFM/SFM approach. For coping with real-
64 world problems that are often a combination of these two situations, the Mixed
65 SFM/OFM and OFM/SFM coupling was therefore developed as a solution (Chang et
66 al., 2015).

67 Sewer inlets are the main interface introducing surface runoff into underground
68 drainage network. Nevertheless, in hydraulic modelling, this process is often
69 simplified or neglected because the details of input data required. The recent
70 improvement of data availability has enabled the possibility to analyse the flow
71 behaviour through inlets and their influence in flood modelling. Shepherd et al.
72 (2012) assess the performance of road gullies through a systematic numerical
73 modelling. Bazin et al. (2014) and Chen et al. (2016) investigated how the flow
74 regime through inlet and manhole changes under different flow conditions and
75 proposed a set of methods to calculate the discharge. Djordjević et al. (2012) and
76 Martins et al. (2014) adopted the Computational Fluid Dynamics (CFD) model
77 OpenFOAM to simulate the flow interaction through a gully, which was compared to

Please cite: *Chang T-J, Wang C-H, Chen AS, Djordjevic S (2018) The effect of inclusion of inlets in dual drainage modelling, Journal of Hydrology. Accepted.*

78 laboratory measurements (different laboratory gullies and OpenFOAM settings were
79 employed in these two studies). Gomez et al. (2016) compared the numerical
80 modelling results, using Flow-3D, with the experimental data to evaluate the inlet
81 coefficient. Lopes et al. (2016) also adopted similar approach to estimate the
82 efficiency of gully with grate slots.

83 In this study, we developed an innovative approach to better simulate the function of
84 inlets during flood events, which was compared to the above-mentioned methods
85 against the measurements in both underground and overland systems of three
86 historical events. The models were calibrated and validated via three flood events
87 with different attributes, i.e. constant moderate rainfall with long duration, intense
88 rainfall with short duration, and extreme rainfall with short duration. The results
89 showed the need to incorporate the new methodology to further improve of modelling
90 accuracy in the Mixed SFM/OFM and OFM/SFM coupling approach.

91 **2 Methodology**

92 **2.1 2D OFM**

93 We adopted and 2D non-inertia OFM to simulate the flood propagation on the
94 ground surface. The 2D OFM is coupled with the Storm Water Management Model
95 (SWMM; Huber and Dickinson, 1988) version 4.4 to simulate the bidirectional
96 interactions between the overland and the sewer systems. Both 2D OFM and
97 SWMM4.4 are developed in Fortran hence they are coupled and compiled as a
98 single code. Assuming the local and convective accelerations are small compared
99 with the gravity and friction terms, the acceleration terms in the SWEs are neglected
100 in the governing equations of the 2D OFM:

$$\frac{\partial d}{\partial t} + \frac{\partial ud}{\partial x} + \frac{\partial vd}{\partial y} = q_s(x, y, t) - q_i(x, y, t) \quad (1)$$

$$-\frac{\partial h}{\partial x} = S_{fx} + \frac{[q_s(x, y, t)]u}{gd} \quad (2)$$

$$-\frac{\partial h}{\partial y} = S_{fy} + \frac{[q_s(x, y, t)]v}{gd} \quad (3)$$

101 where,

d : water depth [m];

t : time [s];

u : velocity component in the x direction [m/s];

v : velocity components in the y direction [m/s];

$h = d + z$: water surface elevation [m];

$$S_{fx} = \frac{n^2 u \sqrt{u^2 + v^2}}{d^{4/3}} \quad \text{: friction slope in x directions [-];}$$

$$S_{fy} = \frac{n^2 v \sqrt{u^2 + v^2}}{d^{4/3}} \quad \text{: friction slope in y direction [-];}$$

n : surface roughness coefficient;

$q_s(x, y, t)$: discharge rate per unit area that the sewer flow surcharges to ground surface [m³/s/m²], considered as point source and determined as

$$q_s(x, y, t) = I + \sum_k \left[\frac{Q_s(x_k, y_k, t)}{A_s(x_k, y_k)} \right] \delta(x - x_k, y - y_k) \quad (4)$$

$q_i(x, y, t)$: discharge rate per unit area that surface water drains to sewer network [m³/s/m²], considered as point sink and determined as

$$q_i(x, y, t) = \sum_k \left[\frac{Q_i(x_k, y_k, t)}{A_i(x_k, y_k)} \right] \delta(x - x_k, y - y_k) \quad (5)$$

I : rainfall excess intensity [m/s];

$Q_s(x_k, y_k, t)$: surcharge discharge determined by SWMM [m³/s];

Please cite: *Chang T-J, Wang C-H, Chen AS, Djordjevic S (2018) The effect of inclusion of inlets in dual drainage modelling, Journal of Hydrology. Accepted.*

$Q_i(x_k, y_k, t)$: drainage discharge to be added to SWMM as the inflow to an inlet of manhole [m³/s];

$A_s(x_k, y_k)$: distributed area of surcharge at the point (x_k, y_k) [m²];

$A_i(x_k, y_k)$: catchment area for inlet at the point (x_k, y_k) [m²];

δ : Dirac delta function

102 In Eqs. (2) and (3), it is assumed that the influx direction of rainfall or manhole
103 effluent is perpendicular to the overland surface and the inlet drainage leaves with
104 overland flow velocity components u and v (Abbott and Minns, 1998). The
105 unknowns d , u and v in Eqs. (1) to (3) are solved by an Alternating Direction Explicit
106 scheme. The derivation of finite difference method for the 2D OFM was depicted in
107 Hsu et al. (2000).

108 **2.2 Interaction between OFM and SFM without gullies**

109 As mentioned earlier, we have developed six approaches in an earlier study of urban
110 flood modelling (Chang et al., 2015). Two of the approaches only involve with 2D
111 OFM and no interaction with 1D SFM is considered. The combined SFM/OFM
112 approach runs the 1D SFM to determine the surcharge discharges from the sewer
113 network, which are used as point sources in the 2D OFM. This is a unidirectional
114 interaction where the surface runoff cannot return to the sewer even when the
115 drainage capacity is available.

116 For the coupled SFM/OFM or OFM/SFM approaches, the interaction between the
117 SFM and OFM is bidirectional such that the runoff can move between the sewer
118 network and the ground surface through manholes or inlets, depending on flow
119 conditions between the two systems. For surcharging condition when the water level
120 in a manhole reaches the ground elevation, the overflow from the sewer network to
121 the ground surface will occur. The discharge from manhole $Q_s(x_k, y_k, t)$ is calculated

122 by the EXTRAN module in the SWMM and assumed to be distributed uniformly in
123 the adjacent area $A_s(x_k, y_k)$ around location (x_k, y_k) and captured by the overland
124 flow model.

125 On the other hand, an inlet at location (x_k, y_k) on the ground surface may collect
126 water from its neighbouring area $A_i(x_k, y_k)$ and drain it to the sewer network through
127 the manhole junction that it is connected to. The drainage capacity $Q_d(x_k, y_k)$ of an
128 inlet depends on its type, e.g., if it is a curb-opening inlet, gutter inlet or grated inlet
129 (Mays, 2011). For low flow rate conditions in both the surface and the sewer
130 systems, the overland flow usually drains fully up to the drainage capacity of the
131 inlet. Hence, the inlet discharge $Q_i(x_k, y_k, t)$ is expressed as follow,

$$Q_i(x_k, y_k, t) = \min \left[A_i(x_k, y_k) \frac{\partial d(x_k, y_k, t)}{\partial t}, Q_d(x_k, y_k) \right] \quad (6)$$

132 where, $d(x_k, y_k, t)$ is water depth [m] at location (x_k, y_k) and time t , $Q_d(x_k, y_k)$ is
133 the design capacity [m³/s] of the inlet at location (x_k, y_k) , which is a given constant.
134 If the manhole that the inlet connects to is not surcharged, the water in the
135 neighbouring area $A_i(x_k, y_k)$ drains with the rate $Q_i(x_k, y_k, t)$ given by Eq. (6). Else, if
136 the manhole is surcharged, which implies that the water is flowing to overland
137 instead of entering sewer, the inlet discharge $Q_i(x_k, y_k, t)$ is set to zero.

138 **2.3 Interaction between OFM and SFM with gullies**

139 In the aforementioned coupled SFM/OFM or OFM/SFM approaches, we simplified
140 the flow dynamic between inlets and manhole, assuming flow transferring from an
141 inlet to a manhole instantly, and the flow interaction between SFM and OFM
142 depends on the flow condition at the manhole. Nevertheless, inlets are connected to

Please cite: *Chang T-J, Wang C-H, Chen AS, Djordjevic S (2018) The effect of inclusion of inlets in dual drainage modelling, Journal of Hydrology. Accepted.*

143 manholes via gullies in reality and the simplification may not reflect the physical
144 phenomena accurately. In this study, we considered the influence of gullies and built
145 a more detailed model with inlets and gullies correctly positioned and connected. As
146 a result, in most conditions the flow exchange between SFM and OFM can only take
147 place at inlets. The only exception is when the high pressure in the sewer network
148 displaces of a manhole cover, thus removing the obstacle for the SFM and OFM
149 flow interaction. An innovative approach for dealing with various flow situations
150 related to manhole cover displacement has been developed by Chen et al. (2016).

151 **3 Model applications and comparison**

152 **3.1 Case study**

153 In this paper, we aimed to compare the two Mixed SFM/OFM and OFM/SFM
154 coupling approaches, i.e. without and with considering the flow process in gullies (as
155 Model A and Model B shown in Figure 1, respectively), and discuss their suitability in
156 modelling practices. We selected the Datong District, a low-lying area in the
157 northwest part of Downtown Taipei, as the case study. The area is located close to
158 the junction where the Keelung River and the Tamsui River meet. Most of the area
159 has an elevation below 5 m above mean sea level, as shown in Figure 2, and the
160 terrain gradually declines from southeast to west, with an average slope of 0.7%.
161 Flood levees on the west side, along the Tamsui River, and on the north side, along
162 the Keelung River, protect the Downtown Taipei from fluvial flooding. The elevated
163 motorway passing the northeast corner of the district forms a closed boundary that
164 connects the two levees along the Tamsui and Keelung Rivers. The area is highly
165 developed, as shown in Figure 3, with 42% covered by buildings, 28% by roads,
166 17% as public open space, and only 13% as green areas. We used a 4m resolution

Please cite: *Chang T-J, Wang C-H, Chen AS, Djordjevic S (2018) The effect of inclusion of inlets in dual drainage modelling, Journal of Hydrology. Accepted.*

167 digital elevation, with a total of 400,000 cells, and a 0.5s time step for 2D OFM, while
168 1s time step was used for 1D SFM.

169 Figure 4 shows the four storm water drainage networks within the area, including
170 1,367 manholes and 29.5 km of pipes, that can cope with intense rainfall up to 1 in 5
171 year return period. Apart from the one (Network 3) in the northwest, the other three
172 (Networks 1, 2 and 4) are connected via three pipes A, B, and C, that allow
173 overflowing from one network to another for easing the burden of the network during
174 extreme conditions.

175 Sluice gates are installed at the outlets of drainage networks that allow for gravity
176 drainage. If the water level in the Tamsui or the Keelung River stops drainage by
177 gravity, the pumping stations are switched on to exclude the storm water to avoid
178 backwater building up in the sewer network(s). The total pumping capacity of the four
179 stations is substantial. Each pumping station has multiple pumps that are operated
180 automatically based on the outer water level in the river and the inner water level at
181 the detention pool. If the outer water level is higher than the inner water level that
182 prevents gravity drainage, pump(s) will be switched on to discharge the sewer flow
183 into the rivers. The number of pumps in operation depends on the water level in the
184 detention pool.

185 The rainfall observations from the Taiping Elementary School (TES) rain gauge, as
186 shown in Figure 4, and the water level records at the network outlets and the water
187 level (WL) gauge in the centre of the whole catchment were used for model
188 calibration and validation. The water level at the network outlets included the river
189 water levels and the ones at the detention pools next to the pumping stations.

190 **3.2 Flood events**

Please cite: *Chang T-J, Wang C-H, Chen AS, Djordjevic S (2018) The effect of inclusion of inlets in dual drainage modelling, Journal of Hydrology. Accepted.*

191 We collected the records of three recent events in 2015 (i.e. 19 July, 23 July and 7-8
192 August) in the case study area for model calibration and validation. We adopted the
193 observations at the TES rain gauges as the rainfall inputs, and the river water levels
194 at the outlets of pumping stations as the downstream boundary conditions. The
195 water level records at the WL gauge and the detention pools were used for
196 calibration and validation. The operation rules of pumping stations, including the start
197 and stop levels of each pump, were applied in the modelling to switch pumps on and
198 off automatically. The modelled hydrographs at the detention pools and the WL
199 gauge were compared to the observed data and evaluated using the Nash-Sutcliffe
200 Efficiency (NSE; Nash and Sutcliffe, 1970). We also adopted the indicators
201 Accuracy, Sensitivity and Precision that were defined as functions of True Positive
202 (TP), False Positive (FP), False Negative (FN) and True Negative (TN) to compare
203 the performance of modelling in terms of overland flood extents. More detailed
204 explanation can be found in Cheng et al. (2015).

$$Accuracy = \frac{TP + TN}{TP + TN + FP + FN} \quad (7)$$

$$Sensitivity = \frac{TP}{TP + FN} \quad (8)$$

$$Precision = \frac{TP}{TP + FP} \quad (9)$$

205 The 7-8 August 2015 event was caused by Typhoon Soudelor that brought in
206 257mm rainfall within 16 hours, as shown in Figure 5(a). The inner water levels
207 started to increase in all four networks after 23:00 on 7 August when the rainfall
208 began. The outer water levels in river channels exceeded the inner water levels at
209 the outlets of Networks 3 and 4 around 01:00, which stopped drainage by gravity and
210 the pumping stations were switched on to discharge the flow from the sewer

Please cite: *Chang T-J, Wang C-H, Chen AS, Djordjevic S (2018) The effect of inclusion of inlets in dual drainage modelling, Journal of Hydrology. Accepted.*

211 networks to the rivers. The outer water levels increased above the inner water levels
212 at outlets of Network 1 and 2 around 1:50 and 02:20, respectively, when the pumps
213 began to work at these two stations. The prolonged precipitation resulted in high flow
214 rates in sewer pipes, which were close to their full capacity in most part of the
215 network, and a minor flooding was reported at one location. However, no detail
216 regarding the flood extent or depth was available. The flow situation of this event
217 was in-between the other two events, and only a minor surface flooding occurred
218 such that the event was used for model calibration.

219 The convective rainfall event on 19 July 2015 dumped 23mm rainfall in the case
220 study area, while 15.5 mm concentrated within 20 minutes as shown in Figure 6(a).
221 The rainfall intensity was below the design rainfall 78.5 mm/h so the sewer networks
222 were able to convey runoff without operating the pumping stations.

223 On 23 July 2015, the area was hit by another storm that brought 125 mm rainfall
224 within 2 hours, as shown in Figure 7(a), with 62 mm concentrated during the peak 30
225 minutes. The sewer networks were unable to cope with such intense rainfall and
226 flooding occurred in several locations. Both events, which represent moderate and
227 extreme conditions, respectively, have complete water level records at the outlets
228 and the WL gauge in the sewer networks so that we adopted the records to validate
229 the modelling results.

230 **3.3 Modelling results**

231 **3.3.1 Model calibration**

232 The modelled water levels at the detention pools of network outlets and the WL
233 gauge using the two Mixed SFM/OFM and OFM/SFM coupling approaches, i.e.
234 (Model A) and (Model B) without and with considering the flow processes in gullies,
235 respectively, of the 7-8 August 2015 event are compared to the observation records

Please cite: *Chang T-J, Wang C-H, Chen AS, Djordjevic S (2018) The effect of inclusion of inlets in dual drainage modelling, Journal of Hydrology. Accepted.*

236 in Figure 8. The peak water levels at the WL gauge were following the peaks of the
237 change of rainfall intensity. The results from both Models A and B captured the trend
238 properly with only slight overestimation during the peaks.

239 The water levels in the detention pools at the outlets from both models were very
240 similar for all four networks. The water level at Network 4 outlet (Figure 8 (e)) varied
241 almost simultaneously with the changes of rainfall intensity with a 10 to 15 minutes
242 delay because the catchment is relatively small and the location of the outlet is very
243 close to the TES gauge. The river water level quickly rose above the water level in
244 the detention pool such that the pump operation played an important role in
245 managing the water level. Four pumps were switched on when the water level at the
246 pool exceeded 0.95m, 0.97m, 1.0m, and 1.02m, respectively. The pumps were
247 operating until the water level reduced to 0.18m, 0.31m, 0.31m and 0.35m,
248 respectively. When the pumps were running, the water level at the pool was
249 dominated by the operation of pumps rather than the rainfall. The same conditions
250 apply to the water level hydrograph at the Network 3 outlet pool (Figure 8 (d)).

251 Due to the larger catchment areas and the longer distances of main trunks, the water
252 levels at outlets of Networks 1 and 2 varied less significantly with the changes of
253 rainfall intensity than the ones in Networks 3 and 4. The water level at Network 1
254 outlet pool (Figure 8 (b)) increased until 01:50, when the river water level exceeded
255 than the pool water level so the pump station began operation. After 05:00, the water
256 level dropped quickly as the result of reduced rainfall and the continuous operation of
257 the pumping station. Similar responses can be found at the Network 2 outlet pool
258 (Figure 8 (c)). The water level changes at the WL gauge (Figure 8 (a)) and the
259 variation of the hydrograph at the Network 2 outlet pool (Figure 8 (c)) show the
260 backwater effect from the downstream. Therefore, the relationship between the

Please cite: *Chang T-J, Wang C-H, Chen AS, Djordjevic S (2018) The effect of inclusion of inlets in dual drainage modelling, Journal of Hydrology. Accepted.*

261 rainfall intensity and the water level at the WL gauge was not obvious. The
262 parameters to be calibrated were the roughness in both the 2D OFM and the 1D
263 SFM. The parameters were adjusted, based on land cover types, and pipe diameters
264 and slopes, and calibrated until the modelled water level hydrographs at all locations
265 were consistent with the observed ones, i.e. NSE was close to 1. The roughness
266 values were determined as (1) 0.02 for roads, plazas, pavements, etc.; (2) 0.08 for
267 green lands, parks, etc.; and (3) 0.05 for built-up areas. The range of roughness of
268 pipes was 0.013-0.018.

269 In general, Model A predicted slightly higher water level than Model B did, especially
270 for the peak values. The NSEs shown in Table 1 indicate that Model B performed
271 better than Model A for the WL gauge and all networks.

272 **3.3.2 Model validation**

273 Figure 9 compares the observed and modelled water level hydrographs at the
274 network outlets and the WL gauge of 19 July 2015 event. The rainfall was not
275 intense and long enough to result in high river levels and to trigger the operation of
276 pumping stations. The records show that the water level at the WL gauge (Figure 9
277 (a)) increased rapidly right after the rainfall started, and reached to the peak level
278 with a 15 minutes lag to the peak rainfall. This reflected the time of concentration at
279 the node for collecting the surface runoff from its subcatchment. After the rainfall
280 stopped, the water level gradually decreased because the coming discharge from
281 further upstream pipes kept the water level high. Both Models A and B produced
282 very similar changing trend but with 0.08m and 0.06m over-estimation of the peak
283 level, respectively. For the water levels at the outlets, the outer water levels dropped
284 below than the ones in pools such that pumping stations were not activated. The
285 sewer flows were slowly discharged to the rivers by gravity, which was also reflected

Please cite: *Chang T-J, Wang C-H, Chen AS, Djordjevic S (2018) The effect of inclusion of inlets in dual drainage modelling, Journal of Hydrology. Accepted.*

286 in the slow declining water level at the WL gauge.

287 Table 2 show the NSEs of the modelled water level hydrographs, compared to the
288 observations. Apart from the outlet of Network 2, which both models produced
289 perfect predictions, Model B performed better than Model A for all locations. The
290 reason for the perfect predictions was that the event was very short such that only
291 limited observation records can be compared to.

292 Figure 10 compares the observation and modelled water level at the network outlets
293 and the WL gauge of 23 July event. The WL gauge records show that the water level
294 increased rapidly right after the rainfall started and stayed at a constant peak level
295 because the full capacity of the network has been reached. The situation lasted for
296 an hour because the coming discharge from further upstream pipes kept the water
297 level high. Then the water level started to decrease, 30 minutes after the rainfall
298 intensity has become lower than the design rainfall intensity. Figure 10 (a) shows
299 that Model A has faster rising and declining limbs of the water level than Model B. It
300 was due to that the flow response time in the gullies was not considered in Model A
301 such that the surface water entered the sewer network more quickly. For the
302 receding part, the water level in Model A began to decrease at eight minutes earlier
303 than the observation, while the Model B result showed a slower timing and pace of
304 water receding. It was due to that Model B was able to capture more surface water
305 through gully inlets from the upstream catchments such that the water level
306 maintained higher than Model A for longer.

307 The water levels at network outlets rapidly increased when the rainfall intensity was
308 above the design rainfall. The operation of pumping station 1 quickly reduced the
309 water level from 13:50. In general, the water level in Model B increased at a slower
310 rate because the flow process in gullies was considered that the runoff collected

Please cite: *Chang T-J, Wang C-H, Chen AS, Djordjevic S (2018) The effect of inclusion of inlets in dual drainage modelling, Journal of Hydrology. Accepted.*

311 from inlets reached to the manhole later than the one in Model A, which assumes
312 that the runoff moves from inlets to manhole immediately. This led to a slower rate of
313 overland flow entering the sewer network, which resulted in later water level increase
314 in the rising part of the hydrograph in sewer network, and a lower discharge of the
315 surcharge flow downstream. Consequently, more water volume stayed in the sewer
316 network such that the water level took longer time to recede, which can be observed
317 in the water level hydrographs. For other networks, the pumps began operating
318 around 13:20 because the continuous rainfall in previous 30 minutes has increased
319 the water levels at the detention pools at WL gauge (a), at the outlet detention pools
320 of Networks 1 to 4 (b-e, respectively).

321 Table 3 shows the NSEs of the modelled water level hydrographs, compared to the
322 observations. Clearly, Model B performed better than Model A for all locations.

323 Although the pumping stations managed to cope with the flow concentrating to the
324 outlets, the upstream pipes of the networks were unable to convey all inflow such
325 that surcharge occurred, as discussed earlier about the condition at the WL gauge.
326 Figure 11 and Figure 12 compare the modelled flood extents to the surveyed one,
327 which was investigated by Taipei City Government after the event, for Model A and
328 B, respectively. The field survey was carried out on the basis of road sections such
329 that the flood extents were delineated along the roads, as a result, the mapped
330 extent may be slightly inconsistent to the real flood situations. Unfortunately, there
331 was no detailed flood depth information attached such that it was not possible to
332 compare the modelled flood depth to the observation.

333 The flood extent in the subcatchments nearby the WL gauge in Model A was smaller
334 than in Model B, but the simulated flood extents from both models were close to the
335 surveyed one. The negligence of the flow process in gullies allowed overland flow to

Please cite: *Chang T-J, Wang C-H, Chen AS, Djordjevic S (2018) The effect of inclusion of inlets in dual drainage modelling, Journal of Hydrology. Accepted.*

336 enter the upstream manhole more easily such that the modelled flood extent was
337 smaller in this area. Same situation occurred in the upstream area of Network 4 (i.e.
338 the flood extent near the bottom boundary), where Model A simulated a smaller flood
339 extent than Model B because the model setting collected more surface runoff from
340 nearby region.

341 For Network 3, the increased upstream flow in Model A led to a greater flood extent
342 along the main road in the east subcatchment. The long road spans the upstream
343 subcatchments of four branches. The flooding in Model A was due to the surcharge
344 water from the second bottom branch that the higher flow in the main trunk affected
345 the runoff entering from this branch. The surcharged water propagated along the
346 main road and flowed southward due to the terrain configuration. In Model B, the
347 gullies could not drain the runoff in the northern part on the same road such that
348 more flooding in that area was simulated. Nevertheless, it reduced the downstream
349 pipe flow such that simulated flood extent in the midstream area in Model B was
350 smaller than in Model A.

351 Table 4 shows the performance of Model A and Model B in predicting the overland
352 flood extent. Both models predicted the flood conditions accurately with 98% of the
353 case study area (Accuracy). However, if we narrow down the area to the surveyed
354 flood extent, Model A only simulated 75% correctly, while Model B performed slightly
355 better at 81% (Sensitivity). In terms of Precision, only 66% and 72% of flood area
356 simulated by Model A and Model B, respectively, was actually flooded. In summary,
357 Model B considered the flow processes in gullies, which enabled it to simulate the
358 interactions between OFM and SFM better and produce results that were closer to
359 the reality.

360 **3.3.3 Modelling costs**

Please cite: *Chang T-J, Wang C-H, Chen AS, Djordjevic S (2018) The effect of inclusion of inlets in dual drainage modelling, Journal of Hydrology. Accepted.*

361 For Model B, extra information regarding gullies were required for setting up. Such
362 detailed data are often difficult or/and expensive to obtain, which is also the main
363 reason why most modelling approaches ignore these elements. Luckily, in the study,
364 we received the information from the Taipei City Government's field survey data. For
365 areas where the surveyed data were absent, we adopted the City Government's
366 storm sewer design standard to set up the inlets and gullies along the road sides in
367 Model B.

368 Table 5 compares the computing time of both Models A and B running on the same
369 desktop computer (with Intel i7-8700 3.7G CPU and 32GB RAM). As expected,
370 Model B required more time for calculating the flow in gullies. Nevertheless, the extra
371 1D SFM computing cost was relatively small, comparing to the 2D OFM part, such
372 that only 1.2 – 3.4% additional cost was incurred to provide better modelling results.

373 **4 Conclusions**

374 In this study, we proposed an improved Mixed OFM/SFM and SFM/OFM coupling
375 approach for urban flood modelling by considering the flow process through gullies,
376 which is often ignored in most OFM/SFM or SFM/OFM coupling approaches. Such
377 detailed process may change the flow dynamic in sewer network and consequently
378 affect the predictions of flood locations and extents. The proposed approach allows
379 better description of the flow dynamic between overland and sewer system flows.
380 The comparisons with the observed water level hydrographs and flood extent in the
381 case study demonstrated that Models A and B can provide reliable modelling results
382 for both moderate and extreme weather conditions, which allows flood risk managers
383 to identify hotspots for developing mitigation measures.

384 **Acknowledgment**

Please cite: *Chang T-J, Wang C-H, Chen AS, Djordjevic S (2018) The effect of inclusion of inlets in dual drainage modelling, Journal of Hydrology. Accepted.*

385 The research is partially funded by the SINATRA project which is supported by the
386 United Kingdom NERC Flooding from Intense Rainfall programme (grant
387 NE/K008765/1).

388 **References**

- 389 Abbott, M.B., Minns, A.W., 1998. Computational Hydraulics, 2nd ed. Ashgate
390 Publishing Limited, The Netherlands.
- 391 Allitt, R., Blanksby, J., Djordjević, S., Maksimović, C., Stewart, D., 2009.
392 Investigations into 1D-1D and 1D-2D Urban Flood Modelling – UKWIR
393 project. Presented at the WaPUG Autumn Conference 2009, Blackpool, UK.
- 394 Arnbjerg-Nielsen, K., 2008. Quantification of climate change on extreme precipitation
395 used for design of sewer systems. Presented at the 11th International
396 Conference on Urban Drainage.
- 397 Balmforth, D., Digman, C., Kellagher, R., Butler, D., 2006. Designing for exceedance
398 in urban drainage – good practice (No. CIRIA C635). CIRIA.
- 399 Bazin, P., Nakagawa, H., Kawaike, K., Paquier, A., Mignot, E., 2014. Modeling Flow
400 Exchanges between a Street and an Underground Drainage Pipe during
401 Urban Floods. *J. Hydraul. Eng.* 04014051.
402 [https://doi.org/10.1061/\(ASCE\)HY.1943-7900.0000917](https://doi.org/10.1061/(ASCE)HY.1943-7900.0000917)
- 403 Bloomberg, M.R., Strickland, C.H., 2012. Guidelines for the Design and Construction
404 of Stormwater Management Systems. N. Y. City Dep. Environ. Prot. Consult.
405 N. Y. City Dep. Build. N. Y. NY USA.
- 406 BSI, 2008. Drain and sewer systems outside buildings - Part 4: Hydraulic design and
407 environmental considerations. British Standards Institution.
- 408 Chang, T.-J., Wang, C.-H., Chen, A.S., 2015. A novel approach to model dynamic
409 flow interactions between storm sewer system and overland surface for
410 different land covers in urban areas. *J. Hydrol.* 524, 662–679.
411 <https://doi.org/10.1016/j.jhydrol.2015.03.014>
- 412 Chen, A., Leandro, J., Djordjevic, S., 2016. Modelling sewer discharge via
413 displacement of manhole covers during flood events using 1D/2D SIPSON/P-
414 DWave dual drainage simulations. *Urban Water J.* 13, 830–840.
415 <https://doi.org/10.1080/1573062X.2015.1041991>
- 416 Chen, A.S., Djordjević, S., Leandro, J., Savic, D., 2007. The urban inundation model
417 with bidirectional flow interaction between 2D overland surface and 1D sewer
418 networks. Presented at the NOVATECH 2007, Lyon, France, pp. 465–472.
- 419 CIWEM UDG, 2016. Rainfall Modelling Guide 2016. CIWEM, London.
- 420 Djordjević, S., Prodanović, D., Maksimović, C., 1999. An approach to stimulation of
421 dual drainage. *Wat Sci Tech* 39, 95–103.
- 422 Djordjević, S., Saul, A.J., Tabor, G.R., Blanksby, J., Galambos, I., Sabtu, N., Sailor,
423 G., 2012. Experimental and numerical investigation of interactions between

Please cite: *Chang T-J, Wang C-H, Chen AS, Djordjevic S (2018) The effect of inclusion of inlets in dual drainage modelling, Journal of Hydrology. Accepted.*

- 424 above and below ground drainage systems. *Water Sci. Technol.* 67, 535.
425 <https://doi.org/10.2166/wst.2012.570>
- 426 Gomez, M., Recasens, J., Russo, B., Martinez-Gomariz, E., 2016. Assessment of
427 inlet efficiency through a 3D simulation: numerical and experimental
428 comparison. *Water Sci. Technol.* 74, 1926–1935.
429 <https://doi.org/10.2166/wst.2016.326>
- 430 Hsu, M.H., Chen, S.H., Chang, T.J., 2002. Dynamic inundation simulation of storm
431 water interaction between sewer system and overland flows. *J. Chin. Inst.*
432 *Eng.* 25, 171–177.
- 433 Hsu, M.H., Chen, S.H., Chang, T.J., 2000. Inundation simulation for urban drainage
434 basin with storm sewer system. *J. Hydrol.* 234, 21–37.
435 [https://doi.org/10.1016/S0022-1694\(00\)00237-7](https://doi.org/10.1016/S0022-1694(00)00237-7)
- 436 Huber, W.C., Dickinson, R.E., 1988. *Storm Water Management Model. User's*
437 *Manual Ver. IV.* U. S. Environmental Protection Agency., Athens Georgia,
438 U.S.A.
- 439 Jahanbazi, M., Egger, U., 2014. Application and comparison of two different dual
440 drainage models to assess urban flooding. *Urban Water J.* 11, 584–595.
441 <https://doi.org/10.1080/1573062X.2013.871041>
- 442 Leandro, J., Chen, A.S., Djordjević, S., Savic, D.A., 2009. Comparison of 1D/1D and
443 1D/2D Coupled (Sewer/Surface) Hydraulic Models for Urban Flood
444 Simulation. *J. Hydraul. Eng.* 135, 495–504.
445 [https://doi.org/10.1061/\(ASCE\)HY.1943-7900.0000037](https://doi.org/10.1061/(ASCE)HY.1943-7900.0000037)
- 446 Leandro, J., Martins, R., 2016. A methodology for linking 2D overland flow models
447 with the sewer network model SWMM 5.1 based on dynamic link libraries.
448 *Water Sci. Technol.* 73, 3017. <https://doi.org/10.2166/wst.2016.171>
- 449 Lopes, P., Leandro, J., Carvalho, R.F., Russo, B., Gómez, M., 2016. Assessment of
450 the Ability of a Volume of Fluid Model to Reproduce the Efficiency of a
451 Continuous Transverse Gully with Grate. *J. Irrig. Drain. Eng.* 142, 04016039.
452 [https://doi.org/10.1061/\(ASCE\)IR.1943-4774.0001058](https://doi.org/10.1061/(ASCE)IR.1943-4774.0001058)
- 453 Martins, R., Leandro, J., Chen, A.S., Djordjević, S., 2017. A comparison of three dual
454 drainage models: Shallow Water vs Local Inertial vs Diffusive Wave. *J.*
455 *Hydroinformatics* 10, 331–348. <https://doi.org/10.2166/hydro.2017.075>
- 456 Martins, R., Leandro, J., de Carvalho, R.F., 2014. Characterization of the hydraulic
457 performance of a gully under drainage conditions. *Water Sci. Technol.* 69,
458 2423. <https://doi.org/10.2166/wst.2014.168>
- 459 Mays, L.W., 2011. *Water resources engineering.* John Wiley, Hoboken, NJ.
- 460 Nash, J.E., Sutcliffe, J.V., 1970. River flow forecasting through conceptual models
461 part I — A discussion of principles. *J. Hydrol.* 10, 282–290.
462 [https://doi.org/10.1016/0022-1694\(70\)90255-6](https://doi.org/10.1016/0022-1694(70)90255-6)
- 463 Rossman, L.A., 2010. *Storm water management model: User's manual Version 5.0.*
- 464 Russo, B., Sunyer, D., Velasco, M., Djordjević, S., 2015. Analysis of extreme
465 flooding events through a calibrated 1D/2D coupled model: the case of
466 Barcelona (Spain). *J. Hydroinformatics* 17, 473.
467 <https://doi.org/10.2166/hydro.2014.063>

Please cite: *Chang T-J, Wang C-H, Chen AS, Djordjevic S (2018) The effect of inclusion of inlets in dual drainage modelling, Journal of Hydrology. Accepted.*

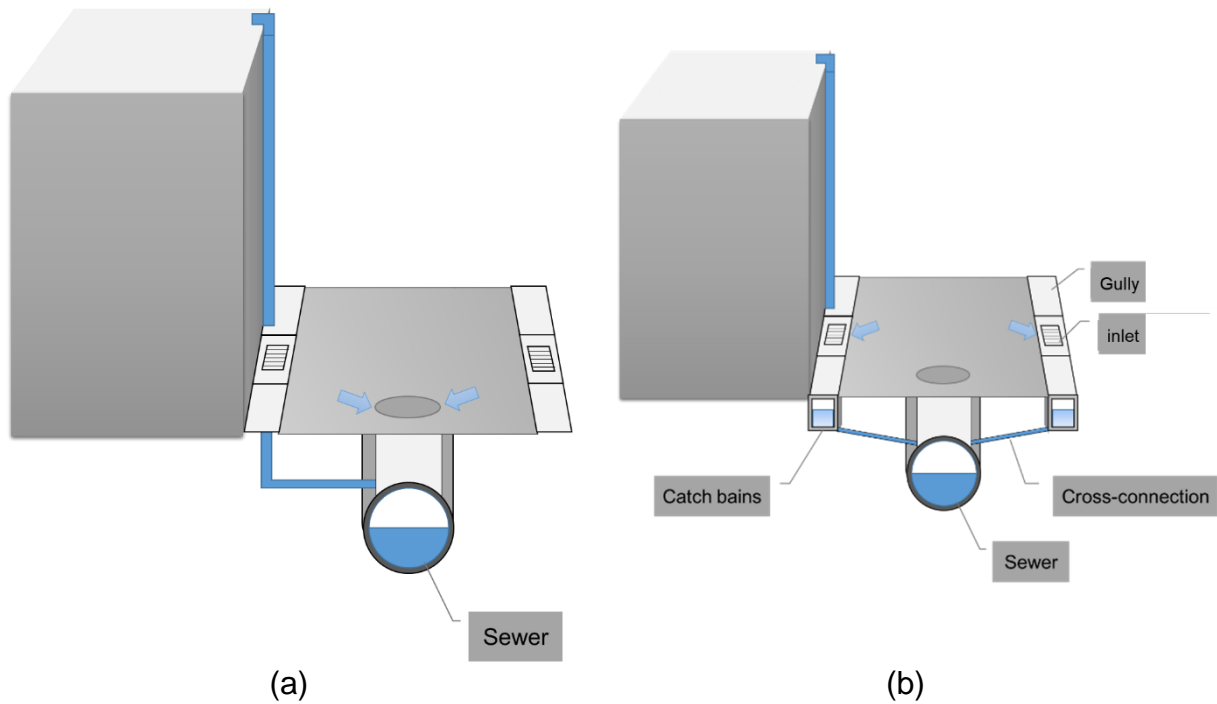
468 Seyoum, S.D., Vojinovic, Z., Price, R.K., Weesakul, S., 2012. Coupled 1D and
469 Noninertia 2D Flood Inundation Model for Simulation of Urban Flooding. *J.*
470 *Hydraul. Eng.-Asce* 138, 23–34. [https://doi.org/10.1061/\(Asce\)Hy.1943-](https://doi.org/10.1061/(Asce)Hy.1943-7900.0000485)
471 [7900.0000485](https://doi.org/10.1061/(Asce)Hy.1943-7900.0000485)

472 Shepherd, W., Blanksby, J., Doncaster, S., Poole, T., 2012. Assessment of Road
473 Gullies, in: *Proceedings of 10th International Conference on Hydroinformatics.*
474 *Presented at the 10th HIC, Hamburg, Germany.*

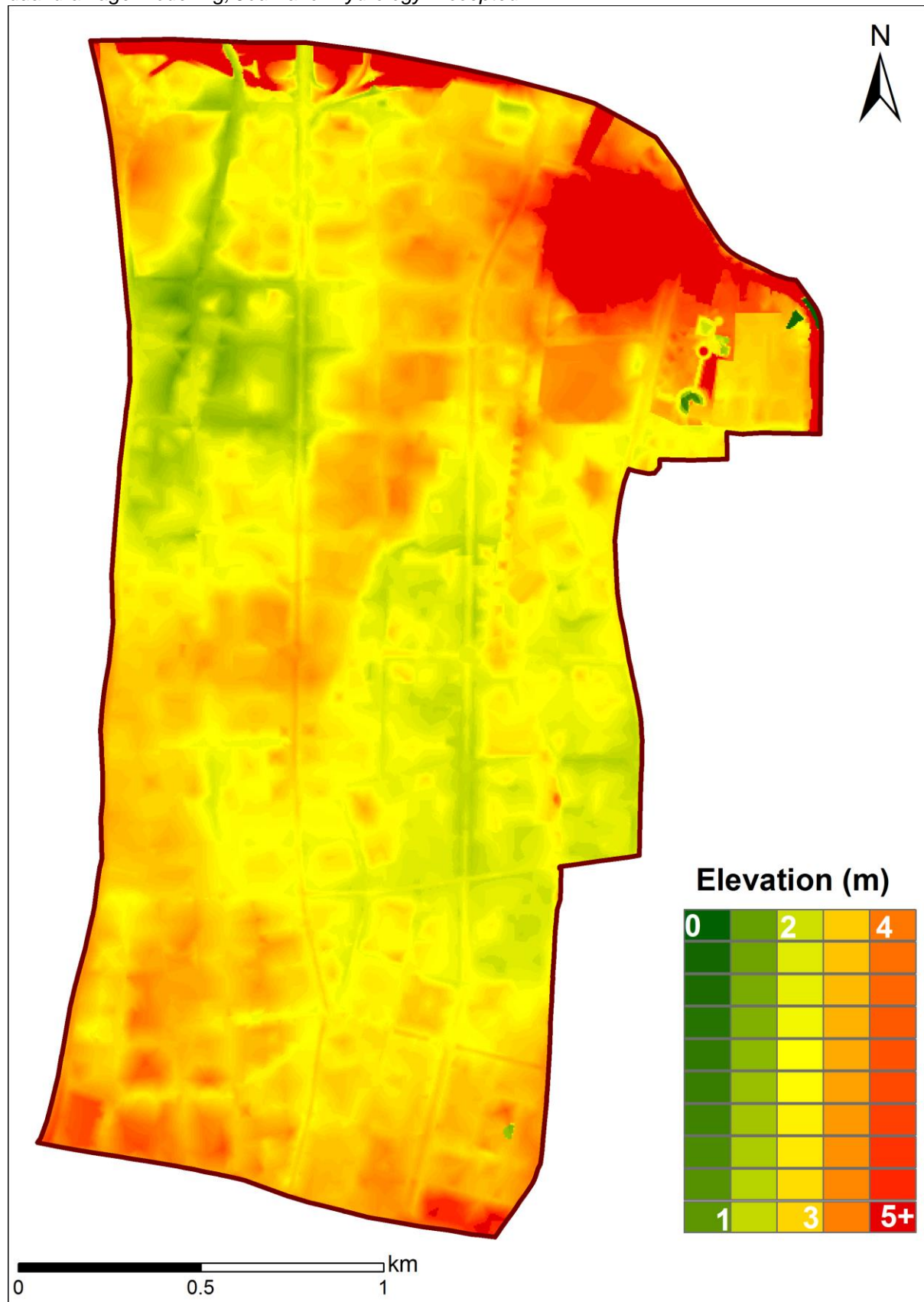
475 Vojinovic, Z., Tutulic, D., 2009. On the use of 1D and coupled 1D-2D modelling
476 approaches for assessment of flood damage in urban areas. *Urban Water J.*
477 *6*, 183–199. <https://doi.org/10.1080/15730620802566877>

478

479 **Figures**

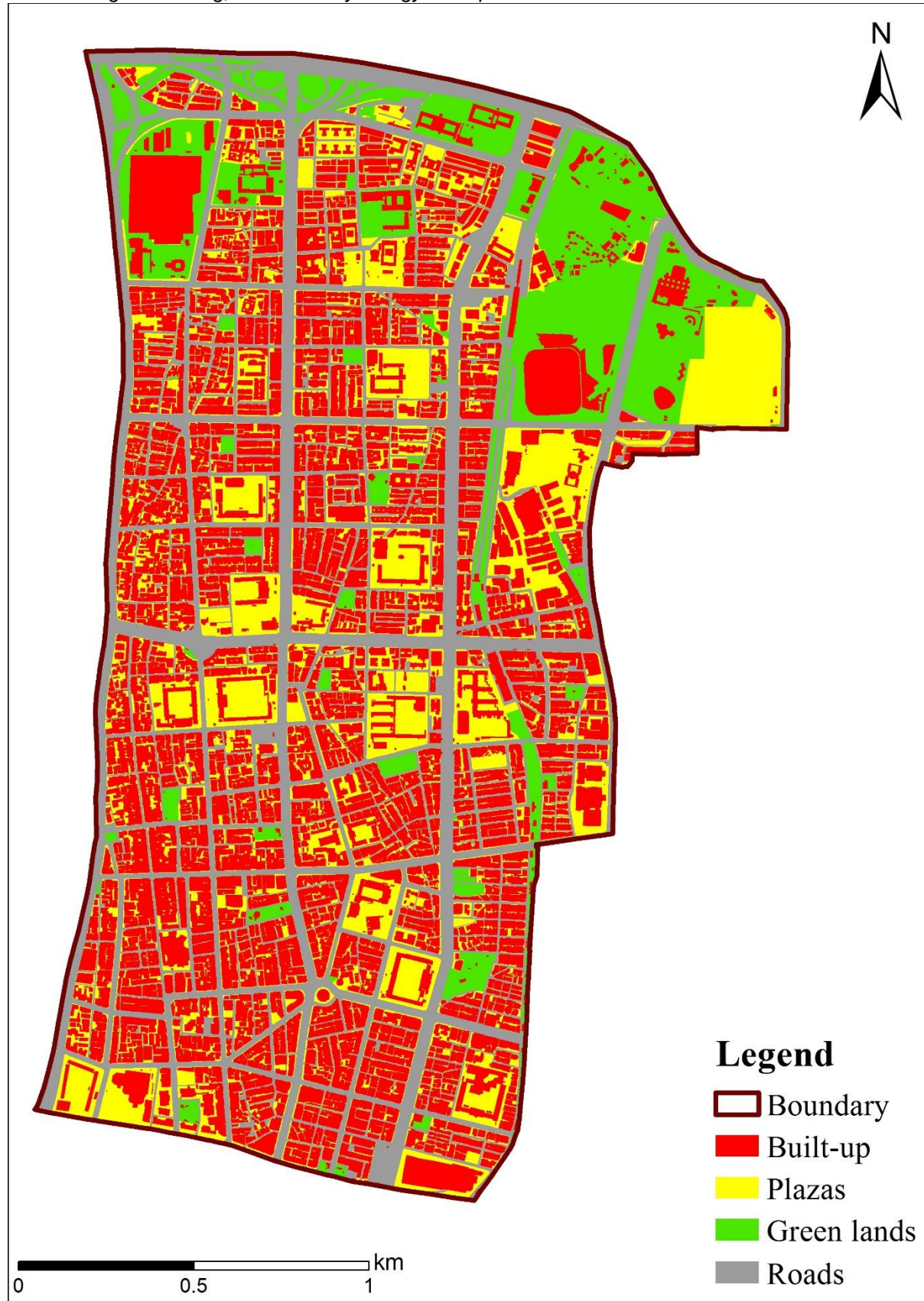


480 Figure 1 Schematic representation of the interaction between 2D OFM and 1D SFM
481 in (a) Model A without gullies (b) Model B with inlets and gullies



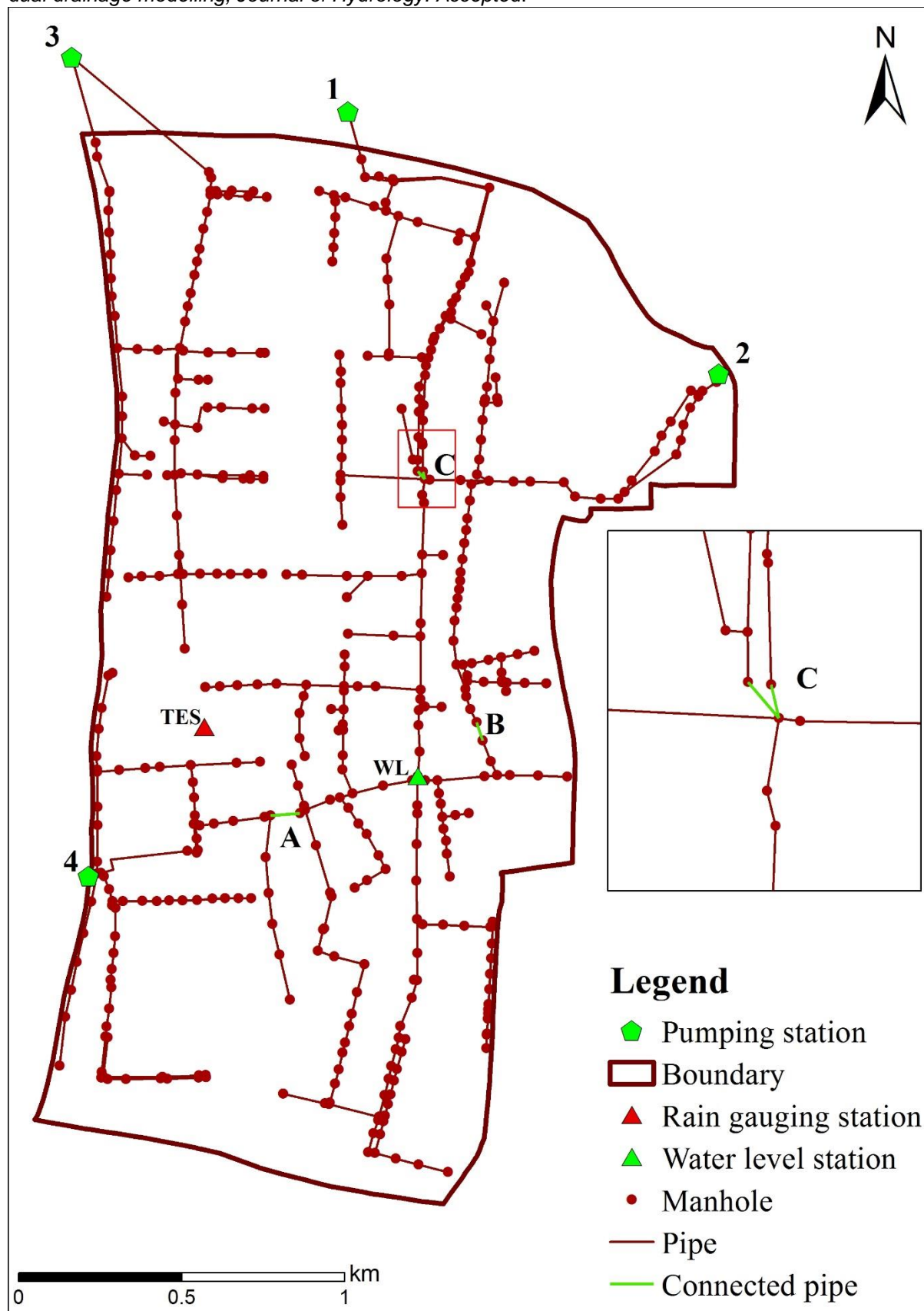
482

483 Figure 2 Terrain elevation of the case study area



484

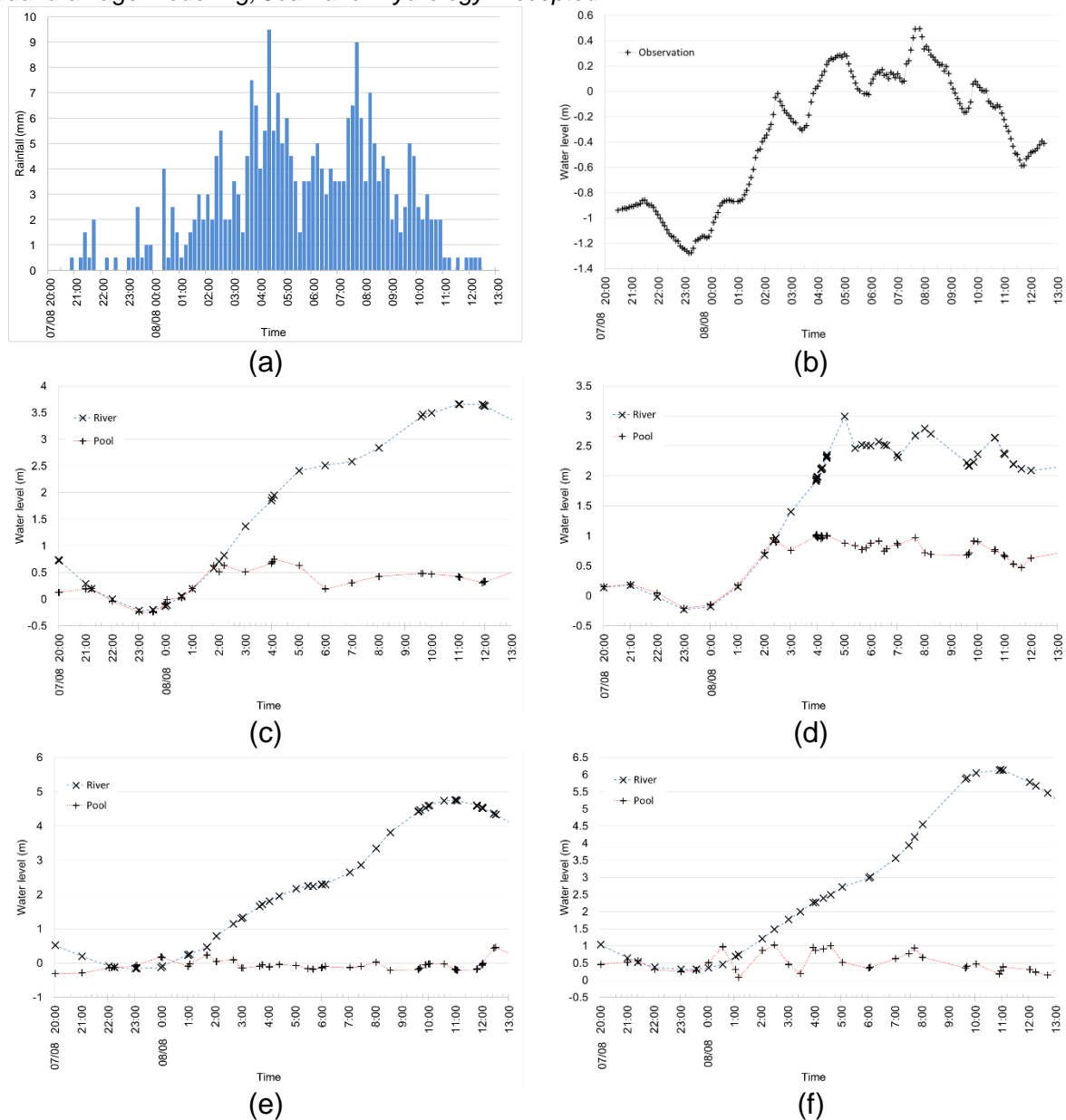
485 Figure 3 Land cover in the case study area



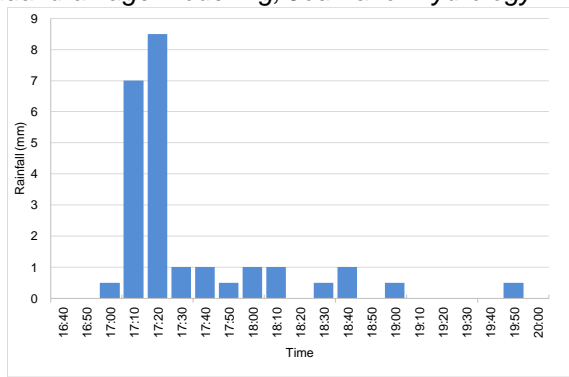
486

487 Figure 4 The drainage network and the locations of the TES rain gauge and the

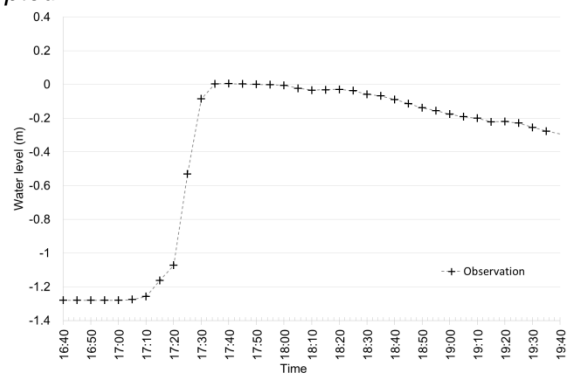
488 water level (WL) gauge in the case study area



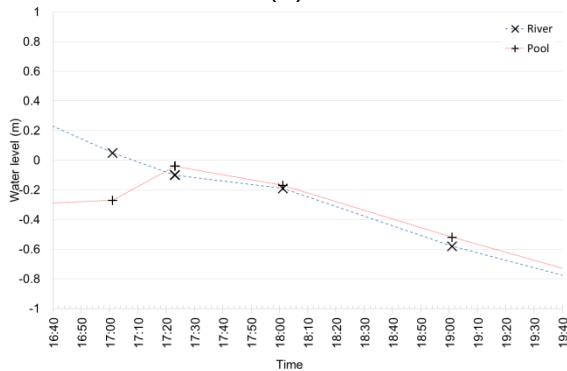
489 Figure 5 (a) The rainfall record at TES rain gauge; and the outer (river) and the inner
 490 (pool) inner and water level hydrographs at (b) at WL gauge; and (c-f) the outlet
 491 detention pools of Networks 1 to 4, respectively, of 7-8 August 2015 event.
 492



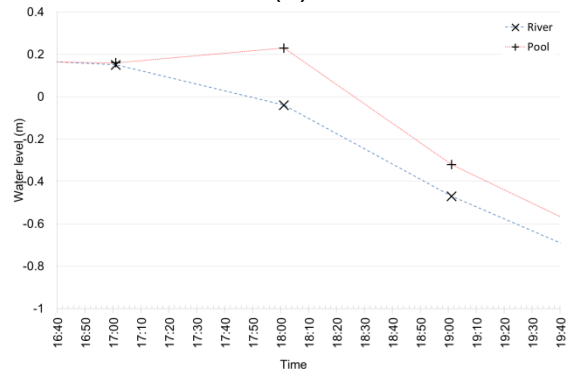
(a)



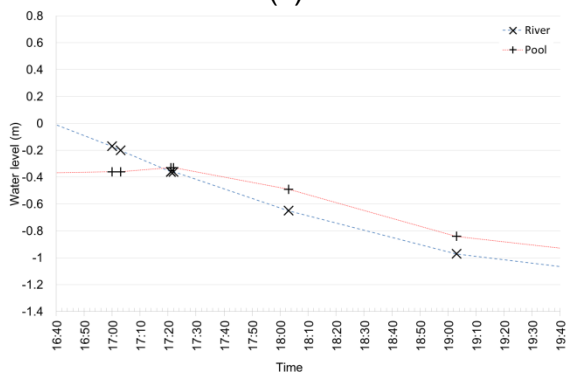
(b)



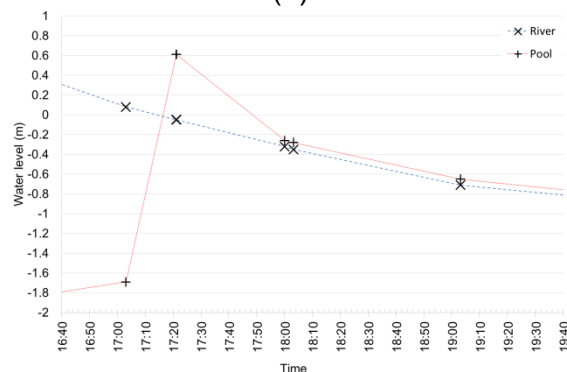
(c)



(d)

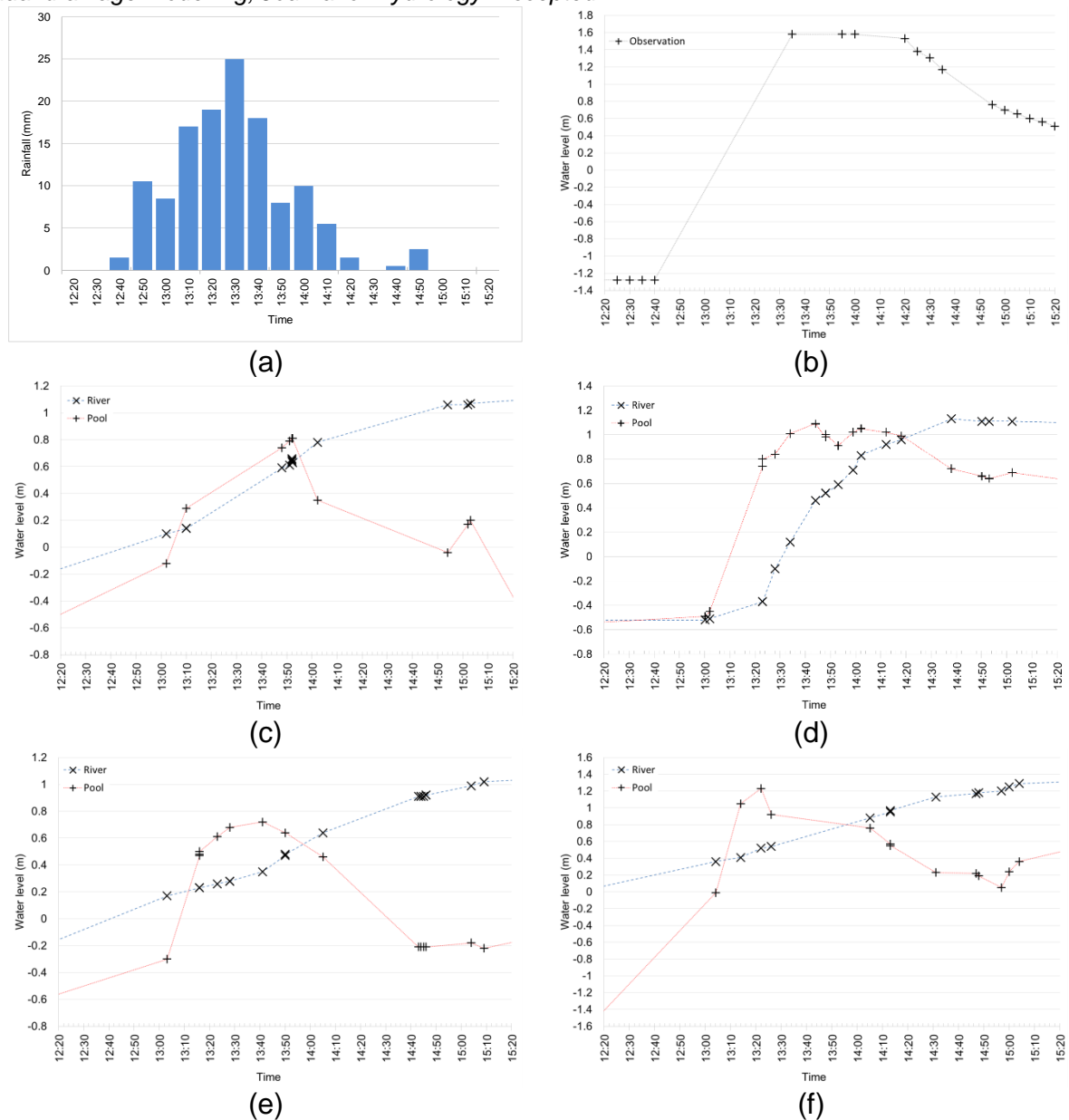


(e)



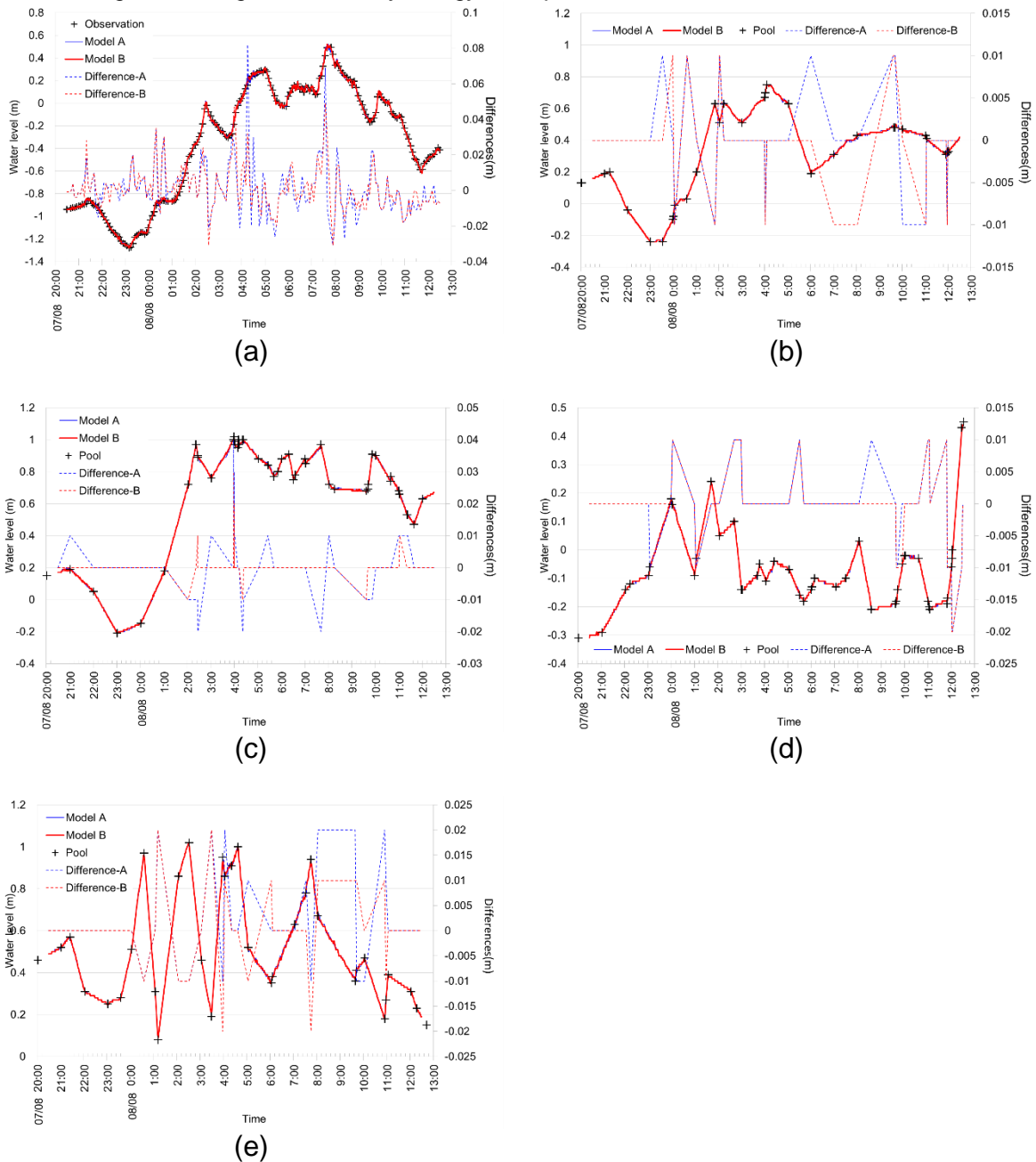
(f)

493 Figure 6 The rainfall record at TES rain gauge; and the outer (river) and the inner
 494 (pool) inner and water level hydrographs at (b) at WL gauge; and (c-f) the outlet
 495 detention pools of Networks 1 to 4, respectively, of 19 July 2015 event.
 496



497 Figure 7 The rainfall record at TES rain gauge; and the outer (river) and the inner
 498 (pool) inner and water level hydrographs at (b) at WL gauge; and (c-f) the outlet
 499 detention pools of Networks 1 to 4, respectively, of 23 July 2015 event.

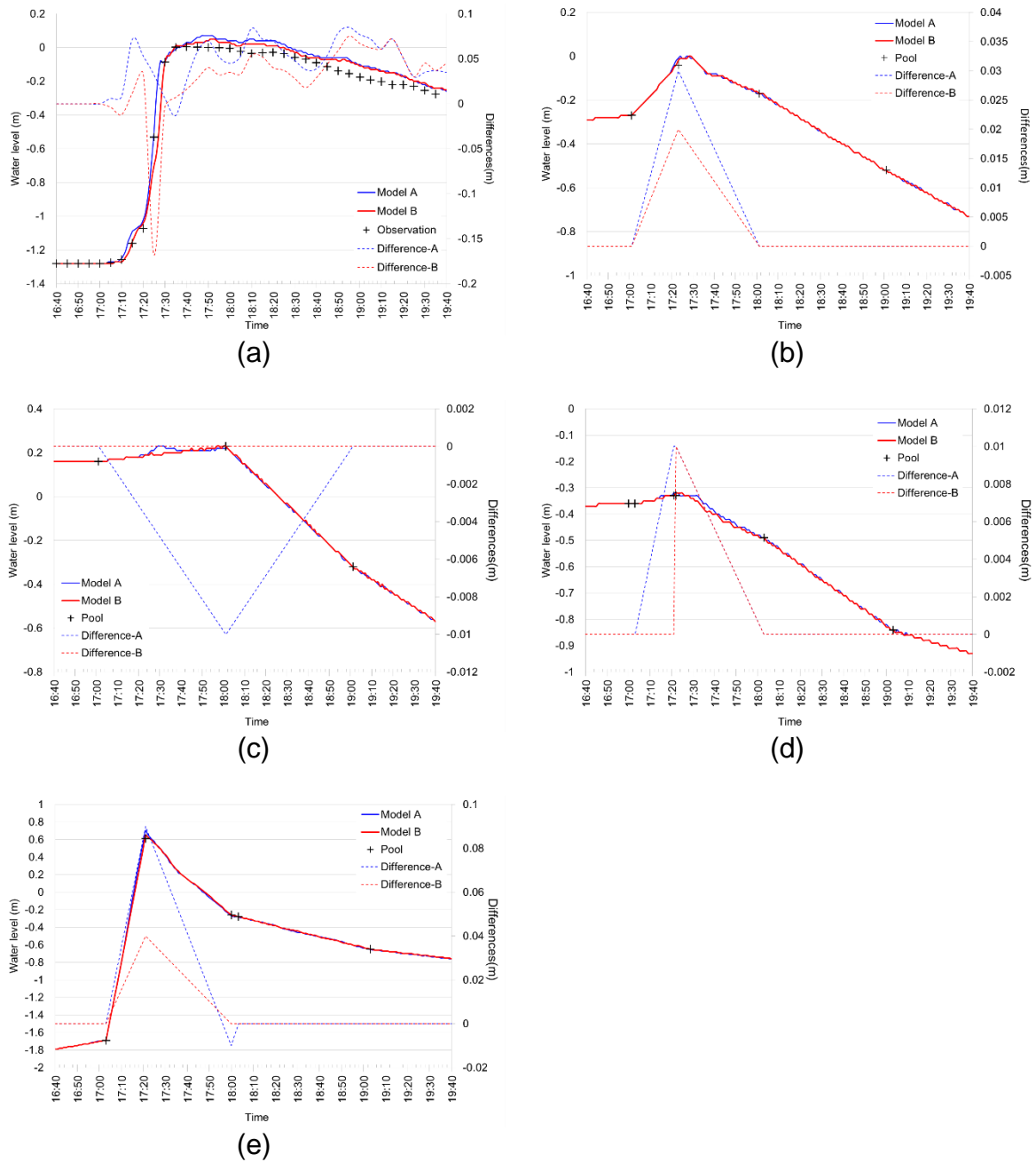
Please cite: *Chang T-J, Wang C-H, Chen AS, Djordjevic S (2018) The effect of inclusion of inlets in dual drainage modelling, Journal of Hydrology. Accepted.*



501 Figure 8 Observed and modelled water level hydrographs of the 7-8 August 2015
 502 event at (a) WL gauge; and (b-e) the outlet detention pools of Networks 1 to 4 (b-e,
 503 respectively).

504

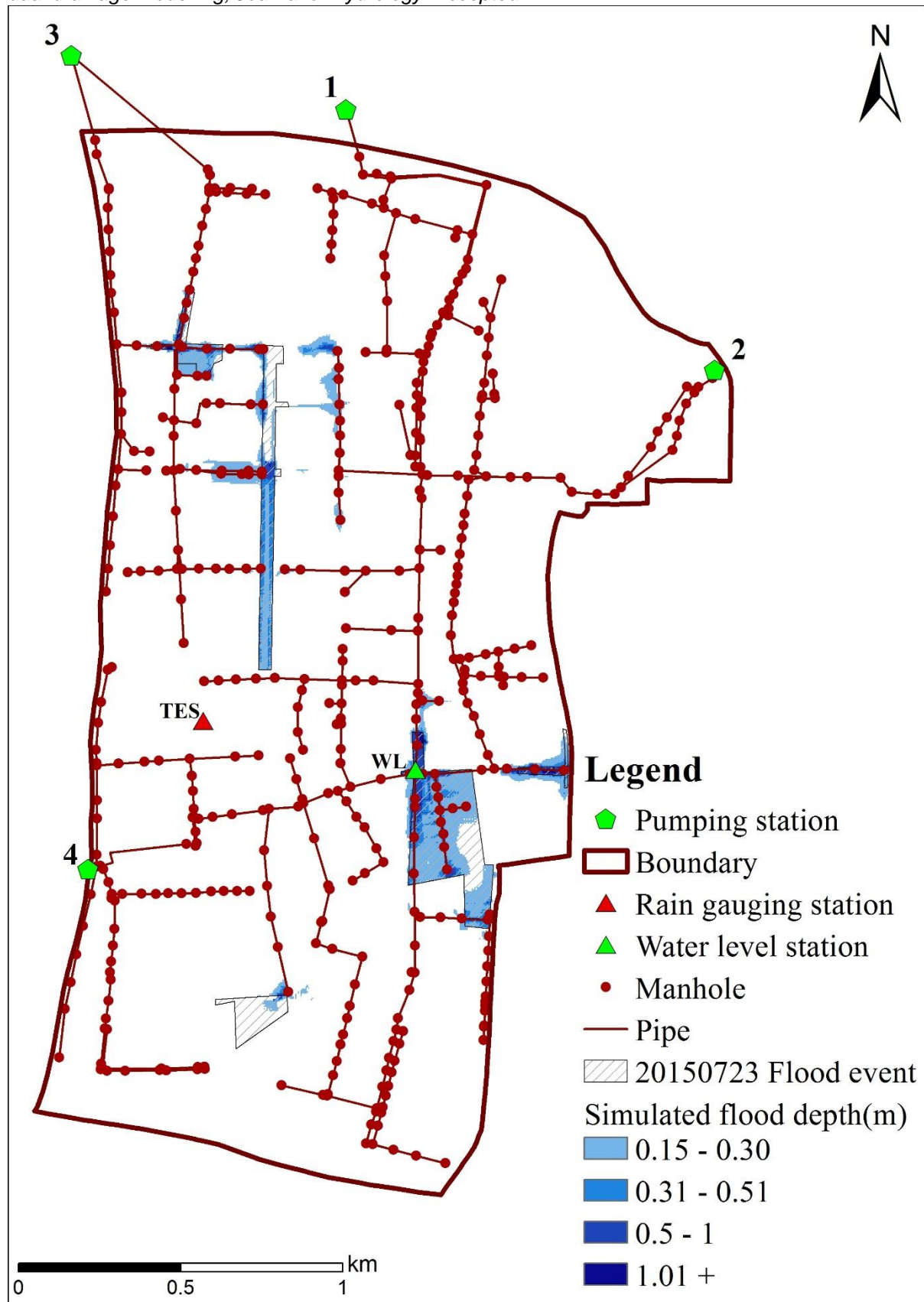
505



506 Figure 9 Observed and modelled water level hydrographs of the 19 July 2015 event
 507 at WL gauge (a), at the outlet detention pools of Networks 1 to 4 (b-e, respectively).
 508



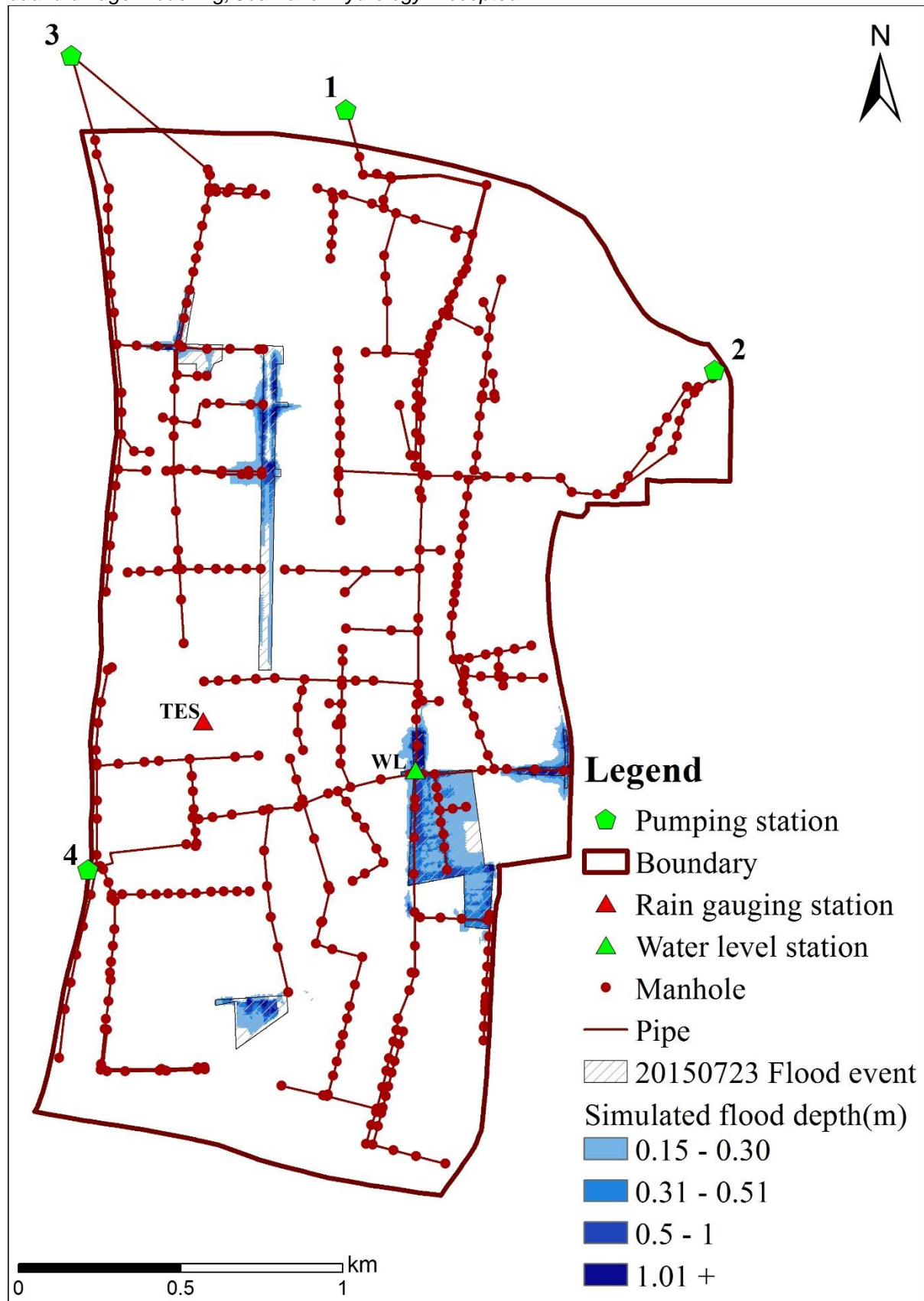
509 Figure 10 Observed and modelled water level hydrographs of the 23 July 2015 event
 510 at WL gauge (a), at the outlet detention pools of Networks 1 to 4 (b-e, respectively).



511

512 Figure 11 Comparison of surveyed and modelled flood extent (Model A) of the 23

513 July 2015 event



514

515 Figure 12 Comparison of surveyed and modelled flood extent (Model B) of the 23

516 July 2015 event

517 **Table captions**

518 Table 1 The NSE of modelled water levels at the network outlets and WL gauge for
519 the 7-8 August 2015 event

Location	Model A	Model B
Network 1 outlet	0.9995	0.9995
Network 2 outlet	0.9991	0.9999
Network 3 outlet	0.9967	0.9968
Network 4 outlet	0.9986	0.9989
WL gauge	0.9992	0.9994

520

521 Table 2 The NSE of modelled water levels at the network outlets and WL gauge for
522 19 July 2015 event

Location	Model A	Model B
Network 1 outlet	0.9927	0.9968
Network 2 outlet	0.9994	1.0000
Network 3 outlet	0.9990	0.9995
Network 4 outlet	0.9970	0.9994
WL gauge	0.9894	0.9907

523

524 Table 3 The NSE of modelled water levels at the network outlets and WL gauge for
525 23 July 2015 event

Location	Model A	Model B
Network 1 outlet	0.9961	0.9976
Network 2 outlet	0.9978	0.9992
Network 3 outlet	0.9981	0.9981
Network 4 outlet	0.9891	0.9901
WL gauge	0.9944	0.9973

526

527 Table 4 The modelling performance indicators

Indicator	Model A	Model B
Accuracy	97.7%	98.1%
Sensitivity	75.1%	81.0%
Precision	65.8%	71.5%

528

529

Please cite: *Chang T-J, Wang C-H, Chen AS, Djordjevic S (2018) The effect of inclusion of inlets in dual drainage modelling, Journal of Hydrology. Accepted.*

530

531 Table 5 The comparison of computing time)

Event	Computing time (s)		Ratio (Model B / Model A)
	Model A	Model B	
7-8 August 2015	13,594	13,753	1.012
19 July 2015	2,267	2,302	1.015
23 July 2015	2,586	2,674	1.034

532